International Journal of Engineering Trends and Technology
ISSN: 2231–5381 / https://doi.org/10.14445/22315381/IJETT-V72I6P127

Volume 72 Issue 6, 287-303, June 2024

Original Article

Experimental Investigation on Performance of High Strength Concrete in Prestressed Hollow Core Slabs Subjected to Elevated Temperature

Jeyashree T M[1], P R Kannan Rajkumar[2]

[1,2]*Department of Civil Engineering, Faculty of Engineering and Technology, SRM Institute of Science and Technology, Kattankulathur, Tamil Nadu, India.*

[1]*Corresponding Author : jeyashrm@srmist.edu.in*

Received: 25 March 2024 Revised: 16 May 2024 Accepted: 08 June 2024 Published: 29 June 2024

Abstract *- The purpose of the study is to examine the effect of elevated temperature on the performance of no-slump high-strength concrete containing fly ash, a routinely utilized material in prestressed precast elements. Assessing the response of structural elements under elevated temperatures is necessary to determine their ability to bear loads under such conditions. Insight into the concrete properties at elevated temperatures can help in assessing the damage attributed to temperature rise on structural elements due to accidental fires or explosions. Three concrete mixes of M50 grade are developed, satisfying the requirement for casting of precast elements by extrusion process. Optimum mix is arrived at room and elevated temperatures by examining the consistency of fresh concrete, and its mechanical and microstructural characteristics. The determined residual properties are compressive strength, split tensile strength, flexural strength, stress-strain behavior, modulus of elasticity, and Poisson's ratio following exposure to a range of temperatures from 100°C to 600°C. Additionally, the established characteristics of the optimum mix are used in examining the post-fire response of prestressed hollow core slab using analytical investigation. The residual properties had a substantial decrease in its value upon reaching a temperature of 400°C and these properties had a major effect on the behaviour of slabs at higher temperatures exhibiting an increase in deflection with the decrease in ultimate load.*

Keywords *- Fly ash, High strength concrete, Elevated temperatures, Residual properties, Hollow core slab.*

1. Introduction

Concrete may experience high temperatures when it is used in industrial applications such as chimneys, reactors, and furnaces and also during accidental fires or explosions [1]. The behaviour of concrete at elevated temperatures is complex, and it depends upon the concrete ingredients, proportions, aggregate type, cement type, porosity, density, and moisture content [2–5]. When subjected to heat, high-strength concrete displays noticeable spalling and has a decreased capacity to absorb moisture compared to standard-strength concrete [6]. Concrete undergoes substantial changes in its thermal, mechanical, and deformation characteristics due to physicochemical transformations occurring during building fires within the temperature range [7, 8]. Concrete's response to high temperatures exhibits significant variability [5, 9, 10], and assessing the structural capacity of concrete in high temperatures is an intricate task [11]. The determined mechanical properties at elevated temperatures by previous researchers on various types of concrete are identified as geopolymer concrete [12–15], self-compacting concrete [16–18], fibre-reinforced concrete [19–22], reactive powder concrete [23] and recycled aggregate concrete [24–26]. Also, researchers focused on examining the impact of temperature rise on compressive strength, split tensile strength, stress-strain curve, microstructural characteristics, and thermal properties. Concrete in high temperatures reveals a variety of behaviours, such as changes in its strength, durability, and structural capacity. The concrete's condition following a fire is typically highly precarious, as it has experienced a loss in stiffness and strength due to temperature rise. Gaining extensive knowledge of these factors and their effect on the prestressed hollow core slabs provides a clearer insight into the thermal effects experienced by slabs during heating.

Therefore, a comprehensive investigation to determine the significant effect of temperature rise on the inherent concrete characteristics and their effects on the performance of prestressed hollow core slabs is carried out. Existing literature indicates a lack of research on the impact of temperature rise on fly ash-based no-slump concrete used in prestressed members. Fresh concrete with a slump of less than 6 mm is defined as no-slump concrete as per ACI 116 (2000) [27]. Zero or no-slump concrete is designated with lesser water content and stiff mix specifically used for the

applications in precast members. Many studies are available to investigate the impact of temperature rise on high-strength concrete with varying concrete ingredients, heating, and testing conditions, and the present study endeavours to investigate the effect of elevated temperatures on high-strength no-slump concrete used in the manufacturing of precast prestressed concrete elements.

Even though the studies, codes, and standards are available to predict the thermal behaviour of concrete at elevated temperatures, it poses a challenge to formulate a comprehensive equation that accounts for the fire and post-fire characteristics suitable for the wide range of concrete types with different heating and cooling rates.

The current investigation aims to ascertain the residual properties of fly ash-based no-slump concrete, and the study is divided into three parts: First, the optimum concrete mix to develop no-slump high-strength concrete arrives at room and elevated temperatures. Second, the impact of temperature rise on concrete properties is investigated, and the results are compared with the available standards and experimental results from previous researchers.

Furthermore, the residual structural behaviour of the prestressed hollow core slab is examined using ABAQUS at both room temperature and elevated temperatures of 400°C, 500°C, and 600°C utilizing the established concrete characteristics at elevated temperature conditions.

2. Materials and Methodology

The post-fire behaviour of concrete used in precast prestressed members is studied by casting and testing the concrete specimens of M50 grade. The concrete mix for precast prestressed members is designed to achieve 70% of the target compressive strength by 18 hours of concrete casting. Generally, concrete used in precast plants is recommended to facilitate the cutting of tendons after 18 hours of casting and the cutting of prestressed members for the required span after 24 hours of casting. Table 1 shows the concrete ingredients used for casting concrete specimens and their properties. The chemical composition of OPC cement of grade 53 and fly ash is shown in Table 2.

Initially, the proportions of concrete ingredients are varied, and the optimum mix to achieve the desired workability and strength is obtained by examining the strength characteristics through a compressive strength test conducted on cubes (100 × 100 × 100 mm), split tensile strength test conducted on cylinders (100 mm diameter and 200 mm height) and flexural strength test conducted on prism (500 × 100 × 100 mm) under three-point loading. The workability of the concrete is determined using the Vee–Bee Consistometer as per ACI 211.3 (2002) [28]. Water curing is used for the present study. The detailed flow of work carried out is given in Figure 1.

Table 1. Properties of concrete ingredients

Material	Properties	Values
Cement	Consistency	31.20%
	Initial setting time	45 minutes
	Final setting time	440 minutes
	Specific gravity	3.15
	Fineness of cement	3.7%
Class F fly ash	Specific gravity	2.2
Fine aggregate	Specific gravity	2.62
	Fineness modulus	3.15
	Zone as per IS 383 (2016)	II
Coarse aggregate	Maximum size of aggregate	10–12.5 mm
	Specific gravity	2.54

Table 2. Chemical composition of cement and fly ash

Composition (%)	Cement	Fly Ash
Calcium oxide (CaO)	61.36	1.97
Silicon dioxide (SiO_2)	22.43	54.90
Aluminium oxide (Al_2O_3)	4.53	27.21
Ferric oxide (Fe_2O_3)	4.42	10.23
Sulphur trioxide (SO_3)	2.39	-
Magnesium oxide (MgO)	1.08	0.82
Sodium oxide (Na_2O)	0.33	1.74
Potassium oxide (K_2O)	0.50	1.78
Loss on ignition	2.97	1.35

2.1. Heating of Specimens

The post-fire performance of concrete is determined by examining the mechanical and micro-structural properties of concrete. The residual properties of the concrete specimens are determined by subjecting the specimen to a certain heating rate until it reaches the desired temperature and reaches a condition of thermal equilibrium. Subsequently, the specimens are permitted to undergo natural cooling, and specimens are evaluated under room temperature conditions to simulate the unstressed residual test condition [29].

The concrete specimens are subjected to gradual heating in a furnace, with the temperature increasing at a rate of 10°C per minute, to achieve the maximum temperature of 100°C, 200°C, 300°C, 400°C, 500°C, or 600°C. The temperature state is transient initially until the target temperature is reached, and then specimens are heated in a steady state for 2 hours. The temperature is maintained for 2 hours for uniform exposure of concrete specimens to achieve a thermal steady state.

Temperature ranges from 100°C to 600°C are used to simulate the pre-flashover and flashover zone of the natural fire curve. The temperature for the flashover zone ranges from 550°C - 600°C [30]. Pre-flashover zone and flashover zone indicate the ignition-growth phase and heating-transition phase of the natural fire curve.

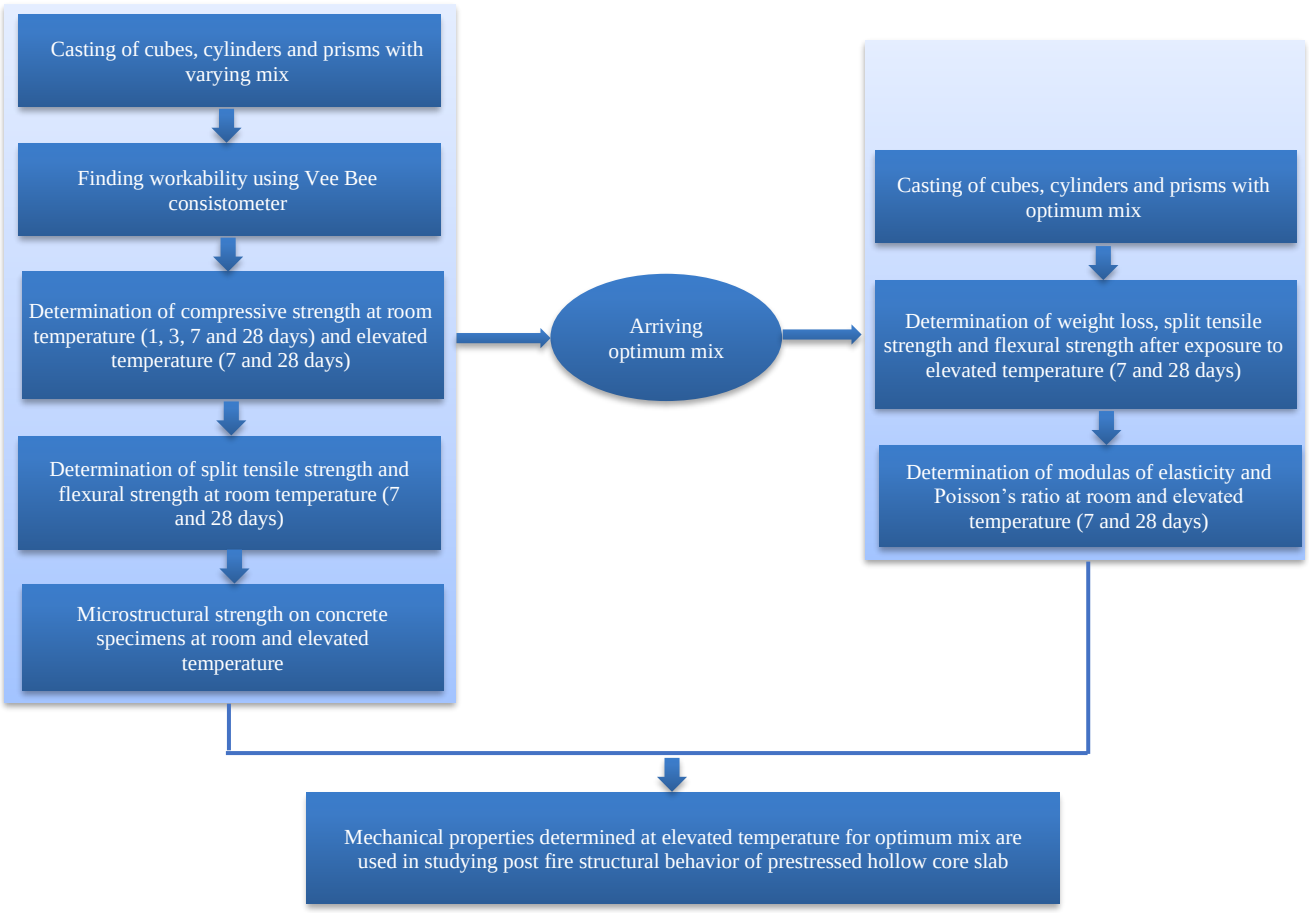

Fig. 1 Outline of the work

3. Mix Design and Experimental Investigation

The concrete mix ratio for the M50 grade is obtained based on recommendations from ACI 211.3 (2002) [28]. The concrete mixes designated as Mix-1, 2, and 3 are varied with concrete ingredients as per the recommendations, and the concrete proportions are given in Table 3. Cohesiveness is an important property required for the casting of precast concrete products to retain the shape after the extrusion process. Aggregate grading and fines in the concrete mixes play a vital role in achieving the desired cohesiveness. Hence, the proportion of aggregate and cementitious materials is varied to achieve the desired requirements. Concrete with a very stiff mix and zero slumps is used in the fabrication of precast elements.

3.1. Consistency of Concrete

The workability is determined by the slump cone test and Vee–Bee consistometer. Vee–Bee consistency of concrete is determined as per ACI: 211.3 (2002) [28] using the Vee–Bee apparatus, and the time taken for the change of concrete shape from cone to cylindrical one is noted down. A dry mix with a lesser amount of water has a higher value of Vee–Bee in seconds compared with the plastic mix. Table 4 gives the types of consistency for different values of slump and the corresponding Vee–Bee seconds.

Table 3. Proportions of concrete ingredients

Material	Quantity of Materials (kg/m^3)		
	Mix-1	Mix-2	Mix-3
Cement	360	380	400
Fly Ash	40	40	40
Fine Aggregate	842	819	979
Coarse Aggregate	998	1021	1028
Water	145	145	145
Super Plasticizer	1.5	1.5	1.5

Table 4. Types of consistency and Vee–Bee in seconds

Consistency Description	Slump (mm)	Vee Bee (Seconds)
Very plastic	125 to 190	-
Plastic	75 to 125	3 to 0
Stiff plastic	25 to 75	5 to 3
Stiff	0 to 25	10 to 5
Very stiff	-	18 to 10
Extremely dry	-	32 to 18

3.2. Mechanical Properties of Concrete

The determined mechanical properties of concrete are compressive strength, split tensile strength, and flexural strength for all three mixes. The residual strength of concrete after heating and cooling to room temperature is determined for 7-day and 28-day cured specimens for all the mixes. A compressive strength test is performed for 1 and 3 days of cured specimens to ascertain the requirement of concrete for casting precast prestressed members. Further strength reduction factor is determined to study the impact of temperature rise on the mechanical characteristics of concrete specimens. The strength reduction factor is determined as the ratio of strength at *t* °C to strength at room temperature. In addition, the modulus of Elasticity (E) and Poisson's ratio are determined for the optimum mix for variations in temperatures from 100°C–600°C by compression testing of cylinders.

3.3. Microstructural Study Using SEM Analysis

Scanning Electron Microscope (SEM) analysis is performed using a high-resolution scanning electron microscope to investigate the impact of elevated temperature on microstructural characteristics of specimens for all three mixes of 28-day cured specimens. SEM images of different scales at 10 and 50 µm are used to observe the microstructural changes occurring in concrete due to temperature rise. The surface morphology is observed for micro-cracks, pores, and voids in the concrete due to temperature rise (100–600°C), and the samples are collected from about 100 mm depth.

4. Results and Discussions

4.1. Preliminary Investigation

As an initial investigation, the optimum mix to achieve the desired workability and strength characteristics is determined by finding the consistency of concrete and compressive strength of concrete specimens at room and elevated temperature. Further, microstructural characteristics are examined to identify the optimum mix.

4.1.1. Consistency of Concrete

The workability of concrete mixes determined by the slump cone test and Vee–Bee Consistometer is shown in Figure 2. The value of the slump measured by the slump cone test is observed as zero mm for all the mixes. Table 5 gives the consistency obtained for concrete mixes, and a very stiff mix to drier mix consistency is recommended for concrete used in precast elements. Mix-1 is observed to be a very stiff mix compared to Mix-2. Mix-3 is an extremely dry mix with a Vee–Bee of 20 Seconds. Mix-1 and Mix-3 meet the required criteria of workability for casting prestressed precast elements.

4.1.2. Mechanical Properties of Concrete at Room Temperature

Table 6 gives the mechanical properties of concrete specimens used for arriving optimum mix. Test results indicate that Mix-3 has achieved greater strength values compared to Mix-1 and Mix-2. The compressive strength development ratio is determined based on the higher target mean compressive strength as per IS 10262 (2019) [51]. The compressive strength development ratio is determined as the ratio of compressive strength determined at the required days to the target mean compressive strength. The target mean compressive strength is evaluated as 58.25 N/mm^2 as per IS 10262 (2019) [51] for M50 concrete grade.

Figure 3 shows the compressive strength development ratio obtained for three mixes and the value is observed higher for Mix-3 compared to Mix-1 and Mix-2. The rate of strength development is observed to be similar for all the mixes with an increase in days, and 73%, 62%, and 60% of target compressive strength is achieved for Mix-3, Mix-2, and Mix-1, respectively, after 24 hours of casting. Also, it is observed that 86% and 99% of the target strength is achieved after 3 and 7 days of curing for Mix-3. The attainment of greater strength for Mix-3 can be due to the densification of concrete mix with proper gradation and optimal packing of aggregates.

Table 5. Consistency for concrete mixes

Concrete mix	Vee Bee (Seconds)	Consistency Description as per ACI 211.3
Mix 1	18	Very stiff
Mix 2	10	Stiff
Mix 3	20	Extremely dry

a) Slump cone test **b) Vee Bee consistency test**

Fig. 2 Measurement of consistency

Table 6. Properties at room temperature

Mechanical properties	No. of days	Values (N/mm^2)		
		Mix - 1	Mix - 2	Mix - 3
Compressive strength	1	35.2	36.3	42.5
	3	40.1	41.4	49.9
	7	46.3	47.6	57.8
	28	50.4	51.8	60.8
Split tensile strength	7	3.83	3.94	4.75
	28	4.21	4.54	4.99
Flexural strength	7	5.37	5.75	6.21
	28	6.01	6.30	6.87

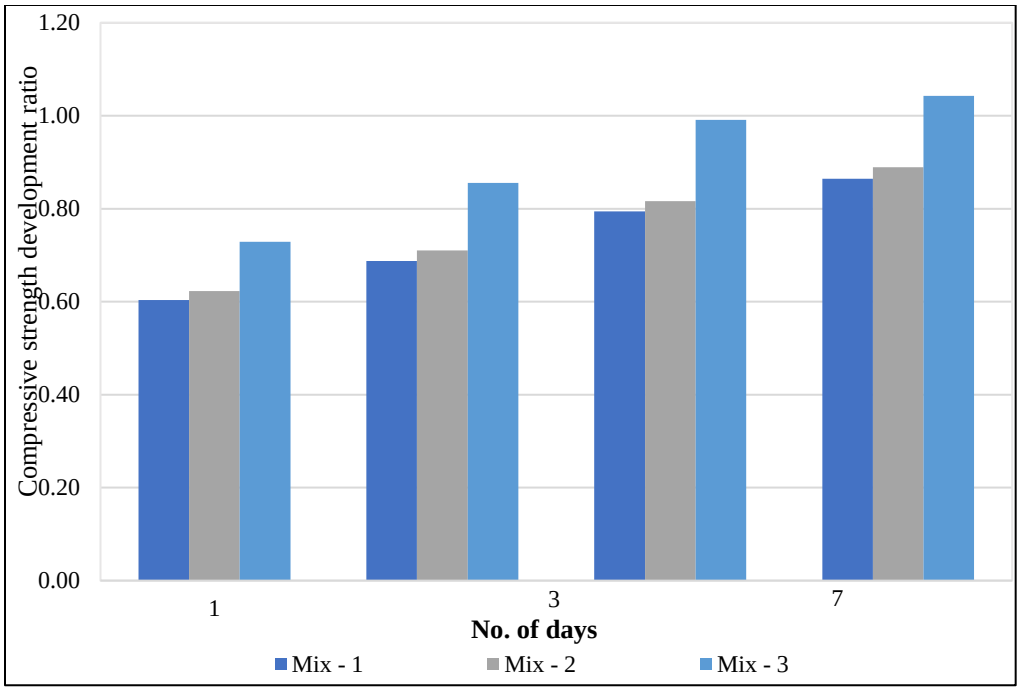

Fig. 3 Compressive strength development ratio

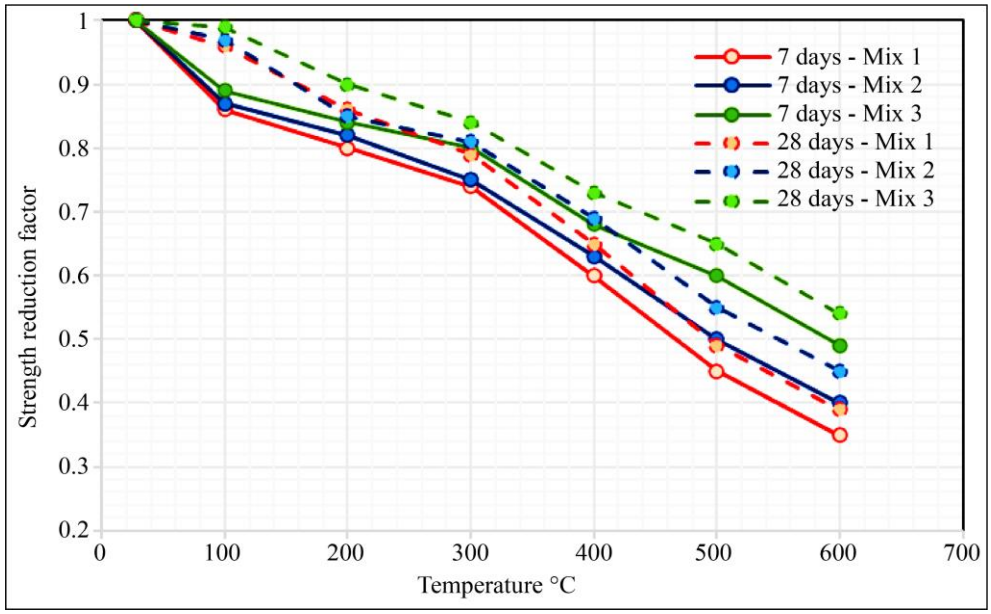

Fig. 4 Compressive strength reduction factor

4.1.3. Compressive Strength at Elevated Temperature

Concrete specimens are exposed to temperatures of 100°C, 200°C, 300°C, 400°C, 500°C, and 600°C for 2 hours after 7 and 28 days of curing. The specimens are placed for heating in a furnace with a maximum temperature capacity of 1200°C. After heating to the required temperature and cooling naturally, the compressive strength test is performed, and the results are given in Table 7 for 7 days of cured specimens. The strength reduction factor is determined as the ratio of strength at *t* °C to strength at room temperature. Based on the test findings, it is inferred that up to 300°C, 16%, 18%, and 20% of initial strength is reduced for Mix-3, Mix-2, and Mix-1, respectively, for 7 days of curing. Beyond 300°C, the strength reduction rate is higher, and at 600°C, only 35%, 40%, and 49% of initial strength are retained for Mix-1, Mix-2, and Mix-3 specimens, respectively, for 7 days of curing. The primary reason for the decrease in compressive strength of concrete when exposed to high temperatures is the loss of water, including both free water and water bound to the cement particles [31, 50].

Table 7. Compressive strength test results for 7 days cured specimens

Temperature *t* °C	Compressive Strength (N/mm^2)			Strength Reduction Factor		
	Mix1	Mix2	Mix3	Mix1	Mix2	Mix3
Room temperature	46.3	47.6	57.8	1	1	1
100°C	39.8	41.4	51.4	0.86	0.87	0.89
200°C	37.0	39.0	48.6	0.80	0.82	0.84
300°C	34.3	35.7	46.2	0.74	0.75	0.80
400°C	27.8	29.9	39.3	0.60	0.63	0.68
500°C	20.8	23.8	34.7	0.45	0.50	0.60
600°C	16.2	19.0	28.3	0.35	0.40	0.49

Table 8. Compressive strength test results for 28 days cured specimens

Temperature *t* °C	Compressive Strength (N/mm^2)			Strength Reduction Factor		
	Mix1	Mix 2	Mix 3	Mix 1	Mix 2	Mix 3
Room Temperature	50.4	51.8	60.80	1	1	1
100°C	48.4	50.2	60.37	0.96	0.97	0.99
200°C	43.3	44.0	54.72	0.86	0.85	0.90
300°C	39.8	41.9	51.07	0.79	0.81	0.84
400°C	32.8	35.7	44.38	0.65	0.69	0.73
500°C	24.7	28.5	39.52	0.49	0.55	0.65
600°C	19.7	23.3	32.83	0.39	0.45	0.54

Table 8 gives the compressive strength and reduction factor for 28 days of cured specimens. Test results infer that exposure of concrete specimens to 600°C resulted in a 61%, 55%, and 46% reduction in initial strength for Mix-1, Mix-2, and Mix-3, respectively. The strength reduction factor is reduced at a faster rate for temperatures greater than 300°C. The decomposition of CSH gel and ettringite occurs at a faster rate when the temperature exceeds 300°C [32, 33], and the strength reduction rate is observed higher for the temperature greater than 300°C for 7 and 28 days cured specimens. Figure 4 illustrates the comparison of the strength reduction factor obtained for Mix-1, Mix-2, and Mix-3 after 7 and 28 days of curing. A similar trend in the rate of strength reduction is observed for both 7 and 28 day cured specimens. 7 days cured and heated specimens are observed to have a higher reduction in compressive strength compared with 28 days cured and heated specimens. Initially, variation in reduction factor for 7 and 28 days of curing is higher up to 200°C for all the mixes, and this can be due to the loss of water required for hydration at initial days for 7 day cured specimens. Once the free water and water from pores get evaporated at lower temperatures (<200°C) from concrete, the variation in the reduction factor remains lower for 7 and 28 days of cured specimens for the temperatures between 300°C to 600°C for all the mixes. Mix-3 is observed to have a greater value of strength reduction compared with Mix-1 and Mix-2 for the temperature range of 100°C to 600°C after 7 and 28 days of curing.

4.1.4. Microstructural Study Using SEM Analysis

Figure 5 shows images of size 10 µm obtained from SEM analysis. The formation of hydrated products with CH and CSH gel is observed in unheated concrete specimens. The initial dense microstructure in the unheated concrete specimens is observed to deteriorate at higher temperatures with the disintegration of CSH and CH gel at 600°C for all three mixes. Micro and macro pores are formed with the temperature rise and significant decomposition of CSH gel is noticed in Figures 5b, 5d, and 5f. The microstructure of concrete is correlated with changes in its mechanical characteristics when subjected to elevated temperature [34], and a higher value of strength reduction is observed at 600°C.

It is observed that Mix-3 has a highly dense matrix compared with Mix-1 and Mix-2. Also, the formation of macro pores is observed less for Mix-3 specimens compared with Mix-1 and Mix-2 after exposure to 600°C. The results are in correlation with the strength test, and Figure 6 shows the microstructure of concrete specimens at 50 µm for Mix-3 subjected to elevated temperatures. CSH decomposition starts when the maximum temperature in concrete is 150°C, and decomposition continues until the maximum temperature reaches 600°C. Beyond 600°C, aggregate damage occurs that initiates the spalling of concrete. At 100°C and 200°C, microcracks and macrocracks are noticed with dense matrix, and at 300°C, decomposition of CSH is initiated, and at

400°C, the partial decomposition of CSH gel is noticed in SEM images. The decomposition of dense matrix is noticed from microstructural analysis with the development of cracks and pores at higher temperatures greater than 300°C. In Figure 6d, cracks are accompanied by the identification of voids with concrete deterioration. At 500°C and 600°C, macro pores and larger size cracks are noticed, which results in a higher value of strength reduction.

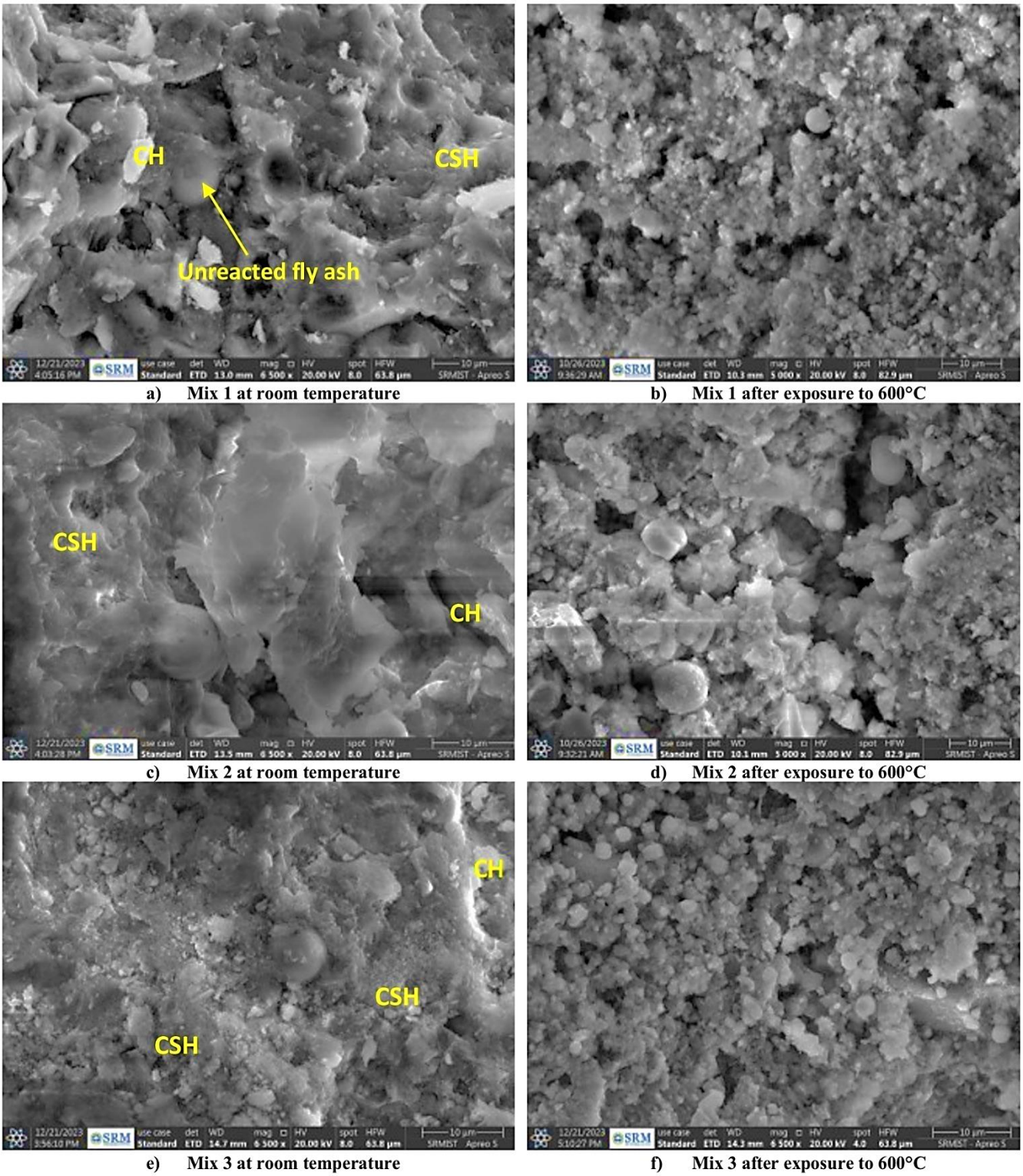

Fig. 5 Output from SEM analysis

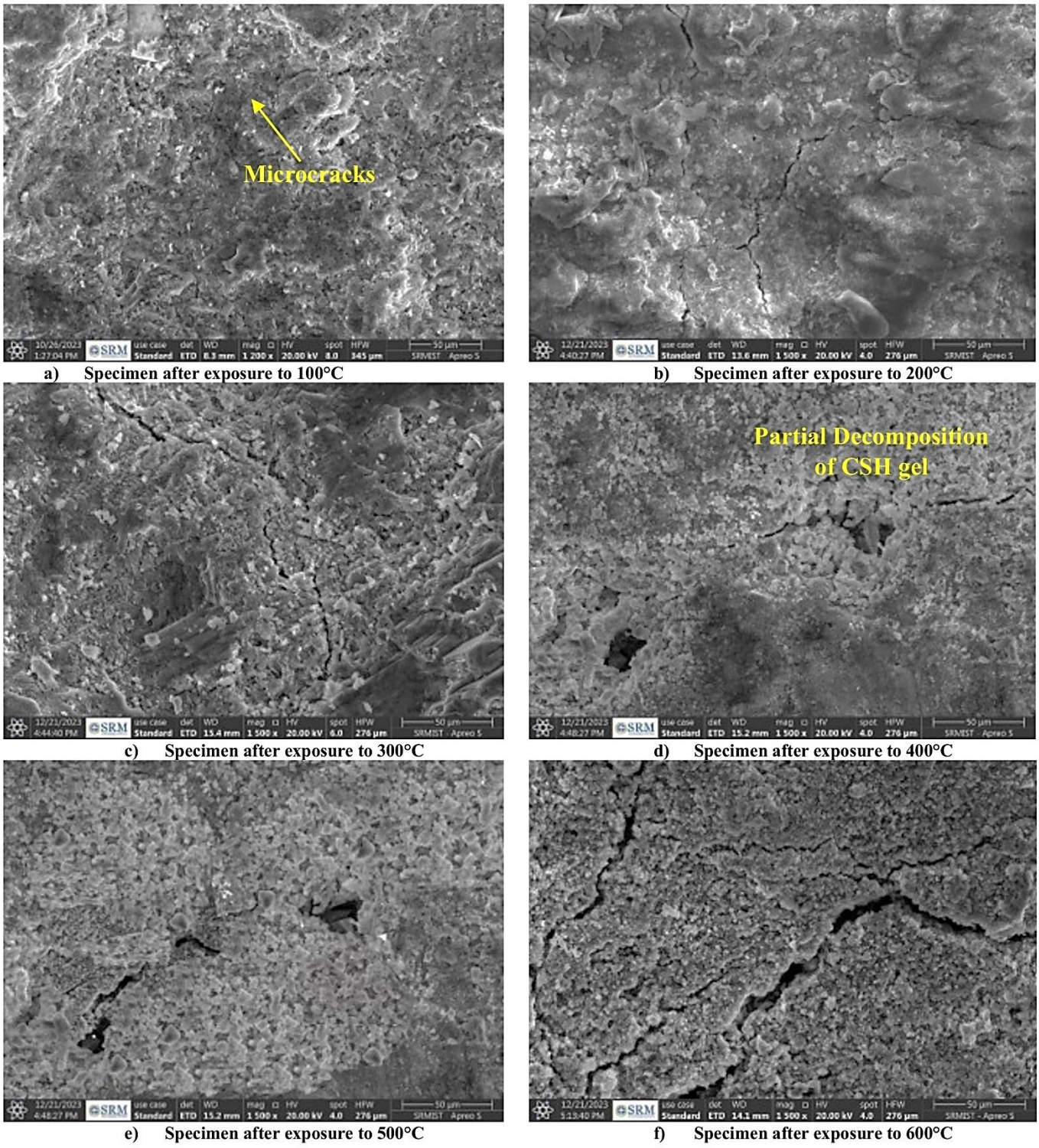

a) Specimen after exposure to 100°C
b) Specimen after exposure to 200°C
c) Specimen after exposure to 300°C
d) Specimen after exposure to 400°C
e) Specimen after exposure to 500°C
f) Specimen after exposure to 600°C

Fig. 6 Output from SEM analysis for Mix-3

4.1.5. Optimum Mix

Based on the examination of workability, strength, and microstructural characteristics of concrete mixes as given, the optimum concrete proportion is Mix–3. Also, it is inferred that the expected design strength for concrete mix is obtained for its recommended applications in precast prestressed members. Further specimens cast with the optimum mix are tested to find the effect of elevated temperature on weight loss, Poisson's ratio, modulus of elasticity, split tensile strength, and flexural strength of specimens.

Fig. 7 Specimens after heating in a furnace

4.2. Properties of Concrete with Optimum Mix

4.2.1. Weight Loss in Concrete Specimens Due to Heating

Figure 7 shows the specimens heated in a furnace for the temperature range of 100°C to 600°C. The weight of specimens before and after heating is determined to examine the impact of temperature rise on the weight loss of concrete specimens. The weight loss (%) in concrete due to temperature rise is given in Figure 8 for cubes, cylinders, and prisms. Percentage loss in weight is observed to be less than 5% after exposure to 100°C for cubes, cylinders, and prisms.

Heating of concrete specimen from room temperature to 100°C, results in loss of free water from concrete [35]. At 100°C, weight loss occurred due to free water loss from pores and resulted in lesser values. Weight loss gradually increased with temperature rise and concrete prisms have undergone lesser weight loss compared to cubes and cylinders. This can be ascribed to the fact that a greater volume of concrete retarded the heating of specimens at higher temperatures. The results are in correlation with the flexural strength test conducted on prisms with lesser values of strength reduction at higher temperatures. Cylinder specimens are observed to have a greater percentage of weight loss compared with cubes and prisms for both 7 and 28 days of cured and heated specimens. The weight loss of specimens after being exposed to high temperatures is associated with the deterioration occurring in the concrete during heating.

4.2.2. Split Tensile Strength

Figure 9 gives the values of the split tensile strength for 7 and 28 days of cured specimens after exposure to elevated temperatures. A greater reduction of tensile strength (<50%) is observed at 500°C, and only 42.9% and 40% of initial strength are retained for 7 and 28 days of cured specimens. Tensile strength shows a consistent decrease up to 400°C; however, after 400°C, a noticeably sharper decrease in strength was observed.

The formation of severe micro and macrocracks caused by thermal stresses and thermal compatible deformation occurring within the concrete are the reasons for this rapid decrease in splitting tensile strength above 400°C [8, 36]. It can be inferred that split tensile strength reduces by 65% and 70% for 7 and 28 days of cured specimens after exposure to 600°C. The split tensile strength of concrete on the 7th day at room temperature is 0.95 times lower than that of the 28th day, whereas, at 600°C, the 7th day strength is 0.82 times lower than that of the 28th day.

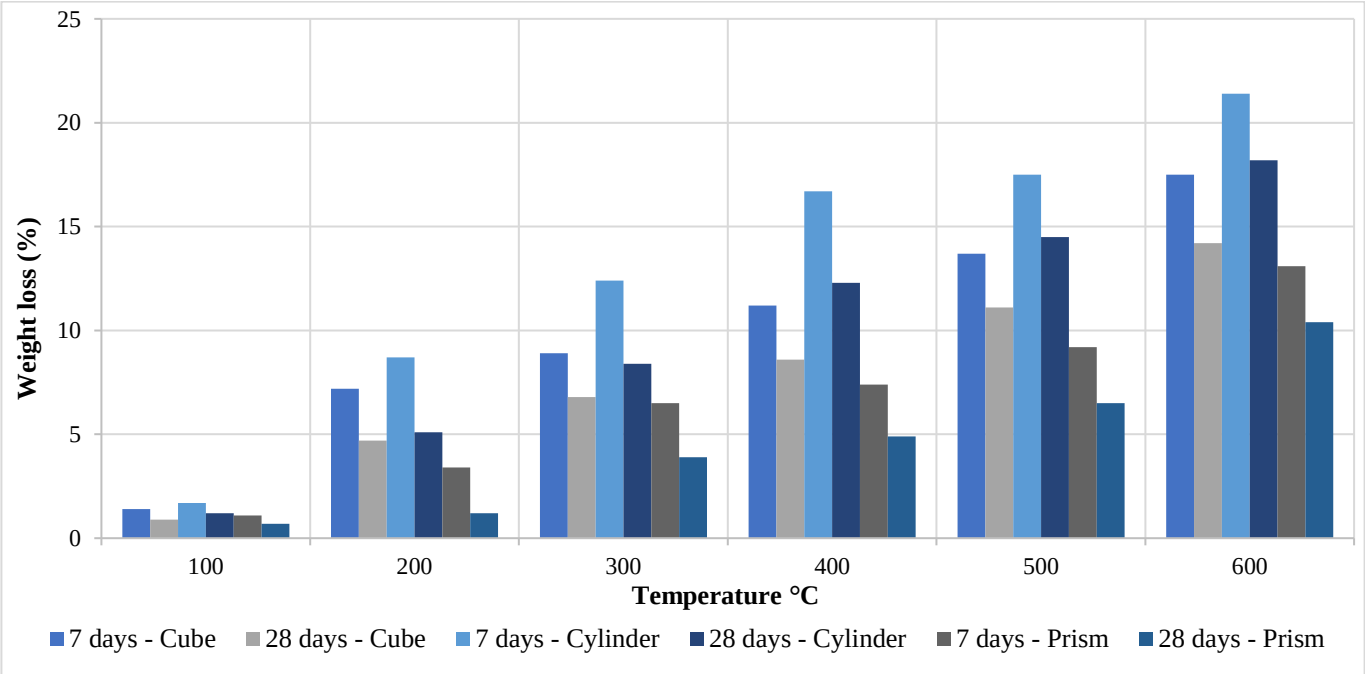

Fig. 8 Percentage of weight loss in concrete specimens

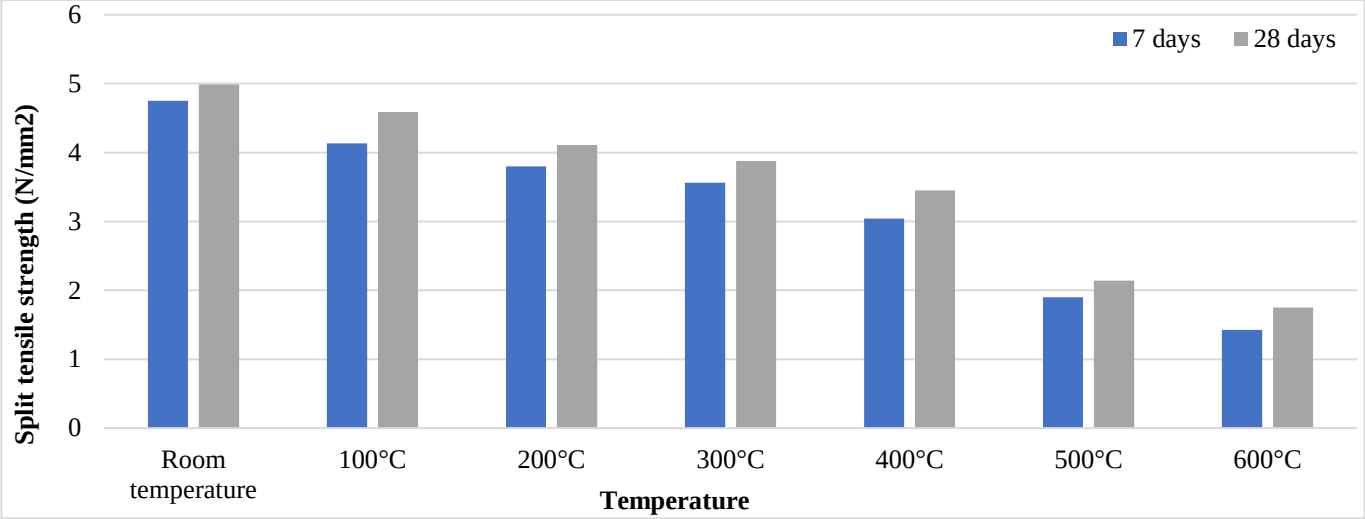

Fig. 9 Results of split tensile strength test

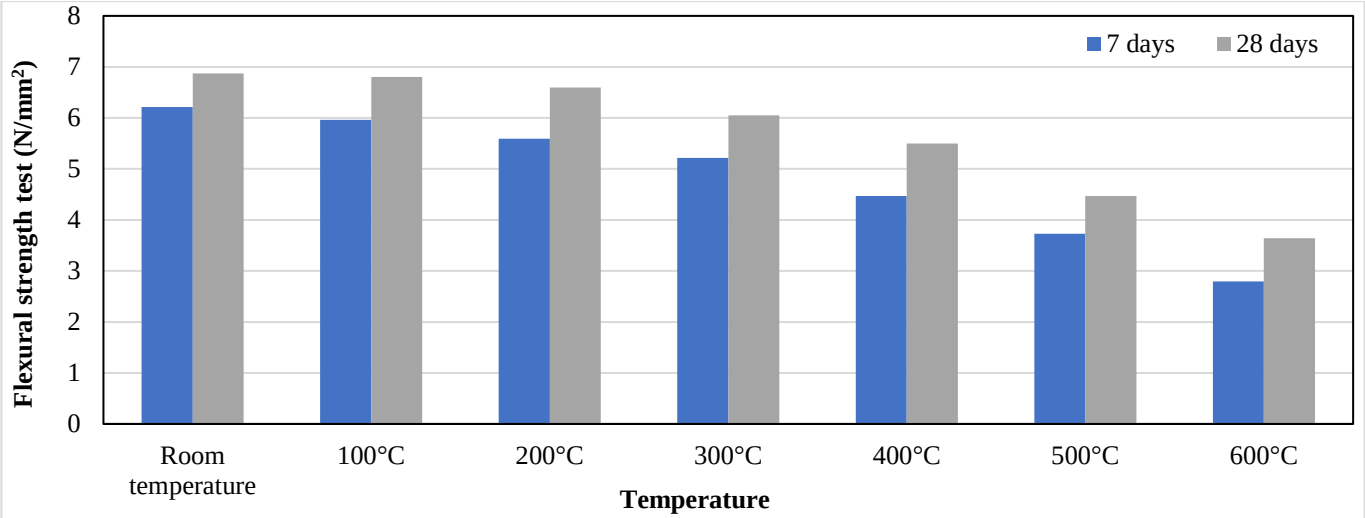

Fig. 10 Results of flexural strength test

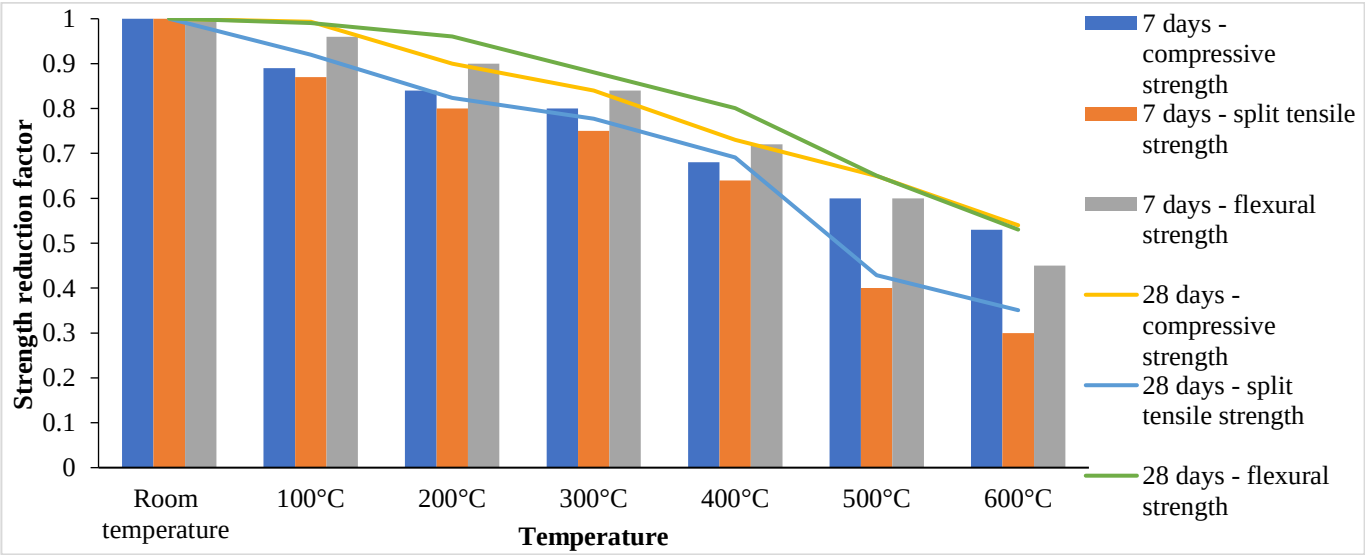

Fig. 11 Comparison of strength reduction factor

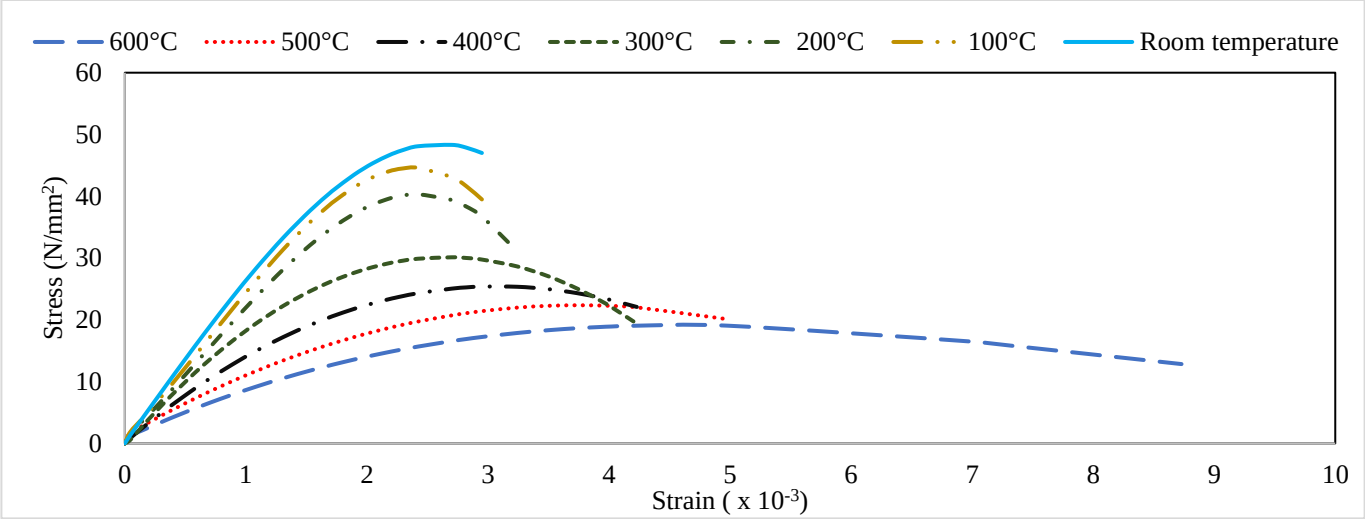

Fig. 12 Stress-strain curve at room and elevated temperatures

4.2.3. Flexural Strength

Figure 10 gives the values of flexural strength obtained for concrete prisms tested at both room and elevated temperatures. Flexural strength test is performed as per IS 516 (1959) [37], and concrete prisms are loaded till failure. Test findings infer that strength decreases with the rise in temperature, and at 600°C, 47% and 55% of initial strength is reduced for 7 and 28 days of cured specimens. Reduction in flexural strength with temperature rise could lead to detrimental effects in beams with greater deflection under elevated temperatures.

Figure 11 shows the comparison of the strength reduction factor determined from the results of compressive strength test, split tensile strength test, and flexural strength test for 7 and 28 days of cured specimens. Split tensile strength is reduced at a faster rate compared with compressive strength and flexural strength. Furthermore, a significant decrease in strength is noticed as the temperature exceeds 400°C for all the test results. It is inferred that 54%, 35%, and 53% of its initial compressive strength, split tensile strength, and flexural strength are retained after heating to 600°C for 28 days cured specimens. Flexural strength is reduced at a lower rate with temperature rise, and this can be due to the retardation of heat by a greater volume of concrete for the same heat exposure condition.

4.2.4. Stress-Strain Curve

Figure 12 illustrates the stress-strain curve under compression for 28 days of cured specimens subjected to room and elevated temperature. The rise in temperature results in a decrease in the slope of the stress-strain curve and peak stress. At 600°C, only 39% of initial stress is retained, and marginal reduction in peak stress is observed up to 200°C, and at 300°C, 62% of initial stress is maintained. The peak strain value corresponding to maximum stress is approximately equal to the initial strain value for the temperature below 200°C. The peak strain exhibits a positive correlation with the increase in temperature beyond 200°C. This can be ascribed to the formation of macropores and cracks in concrete due to thermal stresses experienced at elevated temperatures.

4.2.5. Modulus of Elasticity and Poisson's Ratio

The static modulus of elasticity is determined from the stress-strain curve of concrete under compression as per ASTM C469 (2014) [38]. The residual modulus of elasticity is determined by considering stress equivalent to 40% of the peak load and a longitudinal strain of 50 millionths.

Table 9 gives the values of modulus of elasticity and Poisson's ratio calculated at room and higher temperatures. The ratio of the modulus of elasticity at *t*° C (E_t) to the modulus of elasticity at room temperature (E_r) is determined. Poisson's ratio is calculated based on the transverse strain corresponding to the stress of 40% of peak load and transverse strain of 50 millionths. Transverse strain is measured at the mid-height of the cylinder under compression testing. The ratio of poisson's ratio at temperature *t*° C (μ_t) to poisson's ratio at room temperature (μ_r) is determined.

Table 9. Modulus of elasticity and Poisson's ratio at room and elevated temperatures

Temperature	Modulus of Elasticity-E (GPa)	E_t/E_r	Poisson's ratio (μ)	μ_t/μ_r
Room Temperature	29.099	1	0.23	1
100°C	26.416	0.90	0.20	0.89
200°C	22.683	0.78	0.17	0.77
300°C	20.508	0.70	0.14	0.65
400°C	17.199	0.59	0.10	0.47
500°C	11.700	0.40	0.08	0.38
600°C	8.077	0.27	0.06	0.25

The residual modulus of elasticity is decreased with the rise in temperature and at 400°C, 59% of the initial value is retained. At temperatures beyond 400°C, there is a reduction of almost 50% in the initial value, and at 600°C, only 27% of the initial modulus of elasticity remains. As the temperature rises, the material experiences a disruption in its internal bonds, resulting in a reduction in the elastic modulus and making the material more prone to deformation [39].

Poisson's ratio at room temperature is 0.23 and the values decreased with the temperature rise. The reduction in Poisson's ratio and modulus of elasticity of concrete can be due to the thermal deformation occurring in concrete along with physical and chemical changes.

4.2.6. Comparison of Values of Mechanical Properties with Code Provisions and Existing Results

Figure 13 shows the comparison of the reduction factor for compressive strength obtained from the present study and the estimated values as per EN 1992-1-2 (2004) [40], ACI 216.1 (2014) [41], ASCE Manual (1992) [42], and results from previous researchers [43, 44, 45]. The comparison can assist in suggesting the model for no-slump concrete in the future for specimens heated and tested under unstressed residual conditions. The determined values of the reduction factor for compressive strength from the ASCE Manual (1992) [42], EN 1992-1-2 (2004) [40], and Tanyildizi and Coskun (2008) [43] are higher compared with the present study values. The estimated values by ACI 216.1 (2014) [41] and Malik et al. (2019) [45] are in close correlation with the present study compared with predictions from other standards and experimental results. The variations observed can be due to different methods of heating and heating rate, testing conditions, and concrete mix proportions.

The strength reduction factor determined by the present study can be used for no-slump concrete recommended for application in precast manufacturing plants. However, a detailed investigation is required further to normalize the values for different grades of concrete and mix proportions.

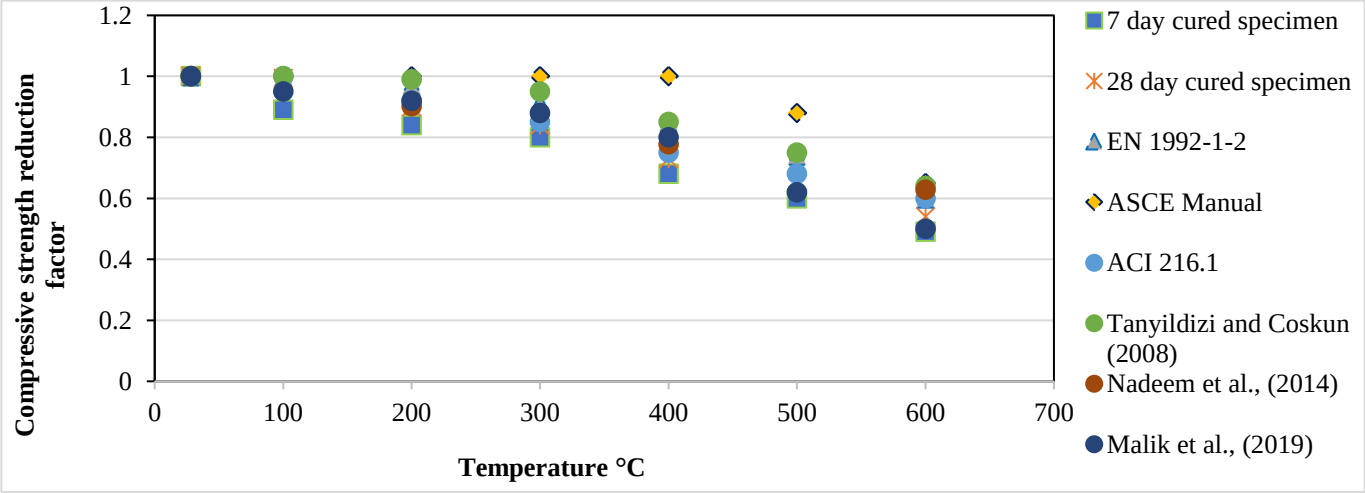

Fig. 13 Compressive strength reduction factor

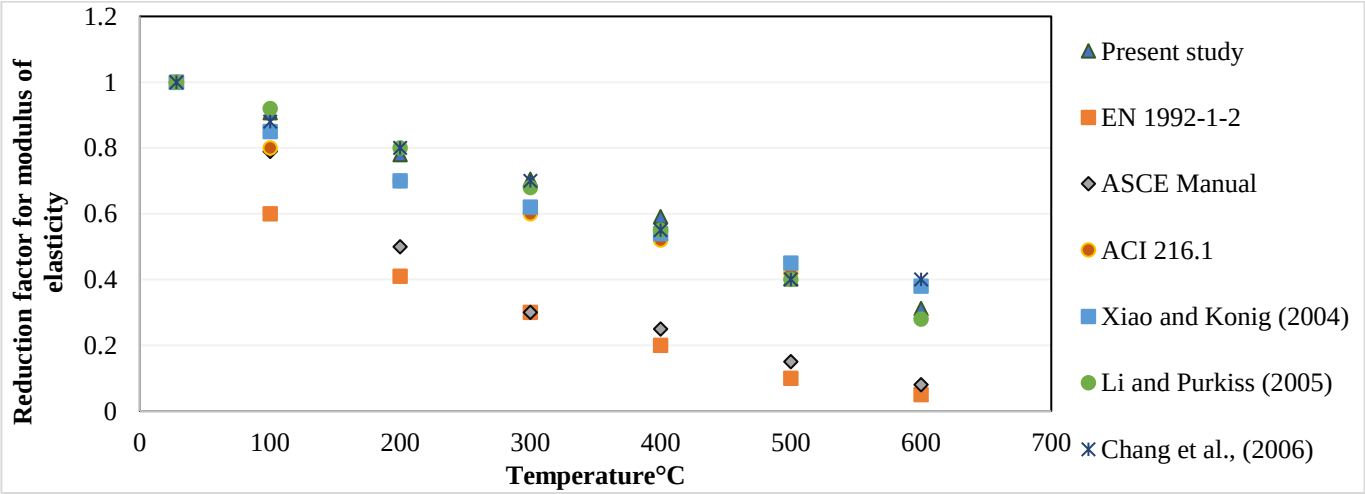

Fig. 14 Reduction factor for modulus of elasticity

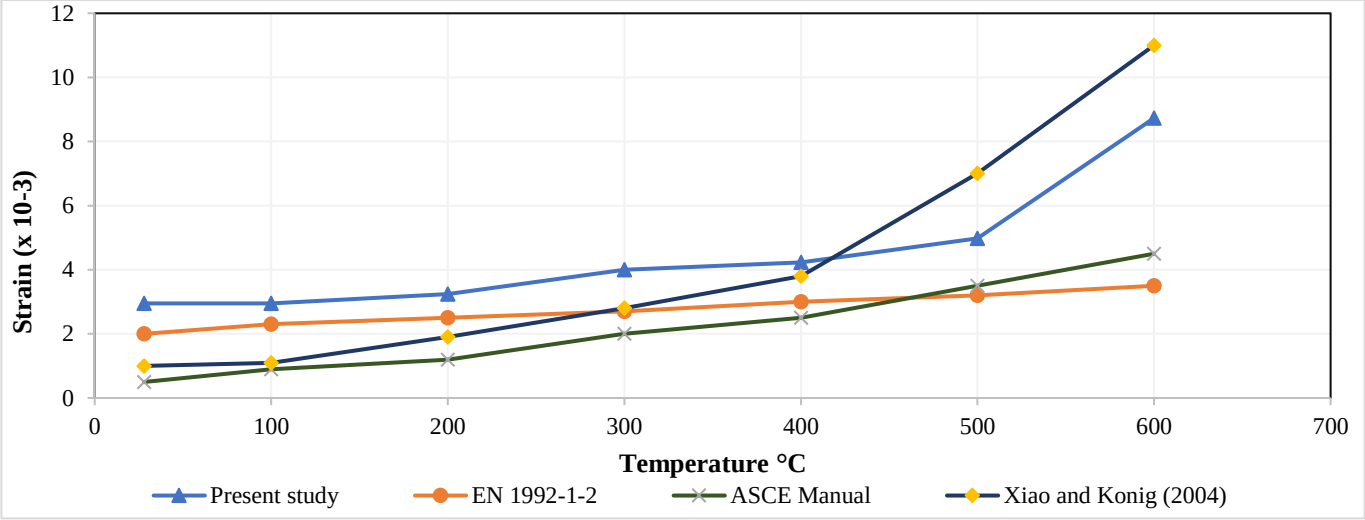

Fig. 15 Comparison of ultimate strain

Figure 14 compares the modulus of elasticity from the present study with the estimated values from ASCE Manual (1992) [42], EN 1992-1-2 (2004) [40], Xiao and Konig (2004) [46], Li and Purkiss (2005) [47], Chang et al. (2006) [48] and ACI 216.1 (2014) [41]. The estimated values obtained from all the codes exhibit substantial deviation from the present study. All of the codes described above significantly estimate the decrease in the elastic modulus at elevated temperatures in the higher range.

The results from the present study exhibit a close correlation with Li and Purkiss (2005) [47] and Chang et al. (2006) [48] for the temperature below 500°C and ACI 216.1(2014) [41] recommendations at 500°C and 600°C. The values from Xiao and Konig (2004) [46] slightly deviated from the present study, and the reduction factor is lesser compared with the present study for temperatures below 400°C.

The comparison of ultimate strain from the present study with the predictions from EN 1992-1-2 (2004), ASCE Manual (1992), and Xiao and Konig (2004) is shown in Figure 15. The maximum strain corresponding to the ultimate stress is examined in this study. The results indicate that the values diverge significantly at temperatures beyond 400°C, with the strain value being particularly larger at 600°C. The residual mechanical properties obtained from the present study can be used as input for the further analytical investigation to investigate the behavior of precast prestressed members under elevated temperatures.

Post-Fire Performance of Hollow Core Slab

The behavior of prestressed hollow core slab subjected to elevated temperature is studied by analytical investigation using ABAQUS 6.14. Finite element modeling and analysis are aimed to simulate the experimental investigation of heating, cooling, and loading till the failure of the slabs. Also, the developed model is used to find the residual maximum load that the hollow core slab can withstand after exposure to elevated temperatures. Temperature gradient and mid-span deflection are determined from the analytical investigation.

The details of the prestressed hollow core slab used in studying the post-fire performance are given in Table 10. An embedded approach simulates the interaction and perfect bond between concrete and prestressing tendons. An 8-node linear heat transfer brick DC3D8 and an 8-node linear brick model with reduced integration and hourglass control C3D84 elements are used in the model to account for heat transfer and stress analysis, respectively. The prestressing force is introduced in tendons by defining the initial stress before the application of load. The boundary condition and loading are applied as specified in Figure 16.

Table 10. Parameters for prestressed hollow core slab

Parameters	Values
Dimension of slab (mm)	4200 × 1200 × 200
Bearing length (mm)	100
Dimension of core	6 numbers of 130 mm diameter
Grade of concrete	M50
Number and diameter of prestressing strands	Six and 12.7 mm
Concrete cover (mm)	40
Grade of strand (N/mm^2)	1860

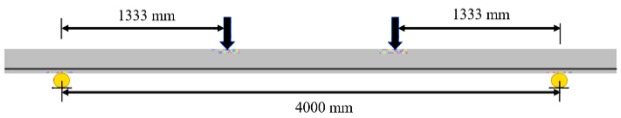

Fig. 16 Loading of slab

Input parameters for concrete are defined based on the experimental results, and the slab is analysed in two cases: i) Analysis at room temperature and ii) Analysis for a maximum temperature of 400-600°C. Concrete's mechanical characteristics experience a more significant decline when the temperature exceeds 400°C. Therefore, the temperature range of 400°C to 600°C is employed to analyse the effect of rising temperature on the system response of prestressed hollow core slabs. The slab is loaded until it fails after being exposed to high temperatures. System response and behaviour are studied by estimating the mid-span deflection. The slab is subjected to heating until it reaches a maximum temperature of 400°C, 500°C, and 600°C. Sequentially coupled thermal stress analysis is used to study the system response. First, thermal analysis is performed, followed by structural analysis. Temperature from thermal analysis is read into the stress analysis by considering the output from heat transfer analysis. Table 11 shows the concrete parameters considered for the analytical investigation. Temperature-dependent properties for steel are given as per EN 1992-1-2 (2004) [40]. The temperature distribution observed on the exposed side of the slabs is given in Figure 17 for heated slabs. Figure 18 shows the results of temperature distribution obtained from the analytical investigation for slab S2.

Figure 19 displays the mid-span deflection of slabs S1, S2, S3, and S4, analysed at both room temperature and increased temperature. Significant deflection is observed in heated slabs, which can be attributed to the inability of the members to tolerate additional deformation caused by thermal effects. The maximum mid-span deflection is compared with the maximum permissible deflection as per ACI 318 (2011) [49] recommendations determined as (span/180) 22 mm. The deflection Of slab S1 is within the allowable limit of 22 mm, with a maximum deflection at failure of 16.78 mm. The maximum deflection observed in slabs S2, S3, and S4 are 21.04 mm, 22.54 mm, and 23.52 mm, respectively, and the deflection accelerated for heated specimens due to a reduction in stiffness and strength of the slabs. Slabs S2, S3, and S4 have an increase in deflection by 25.4%, 34.3% and 40% compared with slab S1. Also, the ultimate load-carrying capacity is reduced for heated specimens compared with unheated specimens. The findings conclude that the deterioration of concrete when exposed to high temperatures has a substantial effect on the structural integrity of prestressed hollow core slabs.

Table 11. Parameters of concrete for analytical investigation

Slab	Maximum Temperature	Compressive Strength (N/mm^2)	E (GPa)	Poisson's Ratio
S1	Room temperature	60.80	29.099	0.23
S2	400°C	44.38	17.199	0.10
S3	500°C	39.52	11.700	0.08
S4	600°C	32.83	8.077	0.06

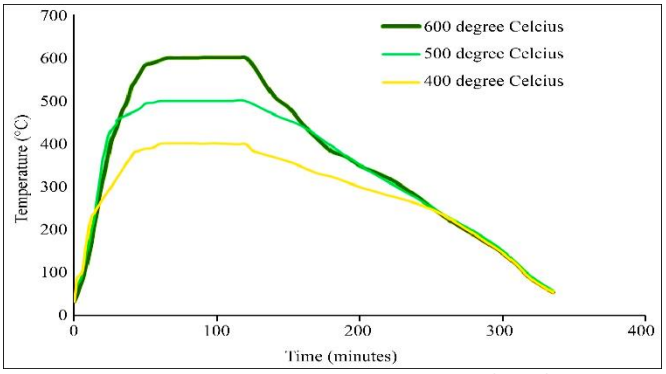

Fig. 17 Temperature predicted on the exposed surface of the heated slabs.

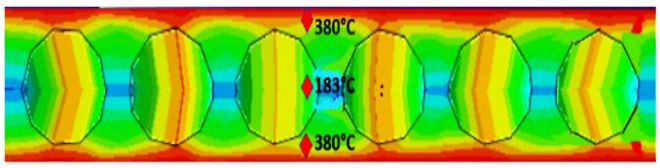

Fig. 18 Temperature distribution for slab S2

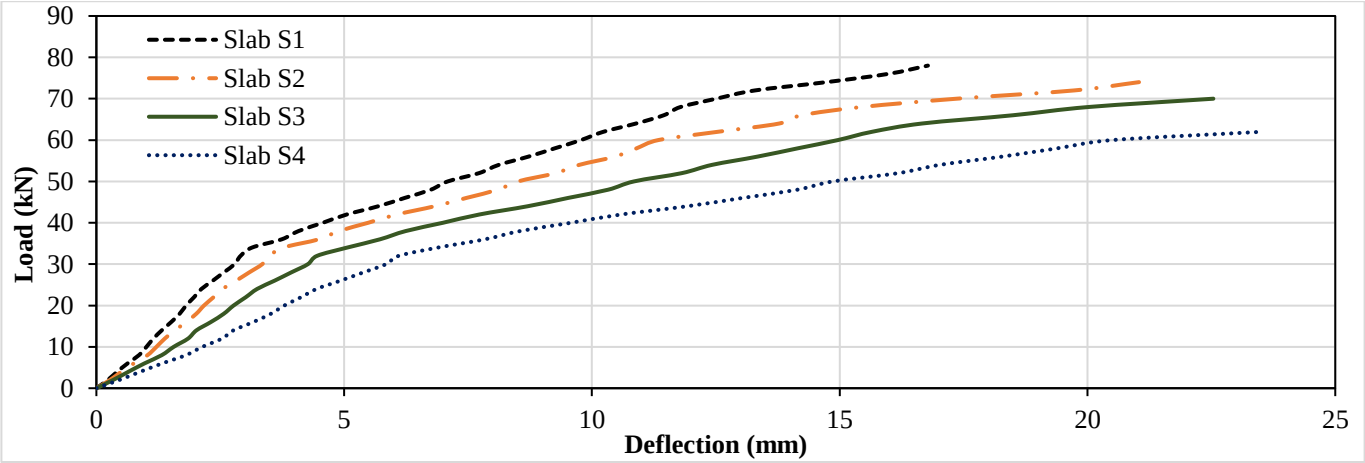

Fig. 19 Load-deflection curve for slabs S1, S2, S3 and S4

5. Conclusion

The conclusions derived from the current investigation are as follows:

- The volume and shape of concrete have a more pronounced influence in elevated temperature circumstances. Cylinder specimens have a greater percentage of weight loss compared with cube and prism for the same heating condition.
- All the specimens with three mixes exhibited comparable compressive strength and responses when subjected to higher temperatures, both at 7 days and 28 days. Upon exposure to a temperature of 600°C, the concrete experienced a significant decline in residual strength, resulting in a reduction in its overall strength on average by 44%.
- The residual split tensile strength had a significant decline in its value after reaching a temperature of 400°C. After being exposed to temperatures of 500°C and 600°C, only 43% and 35% of its initial strength are retained.
- The values of flexural strength at elevated temperatures are similar to compressive and split tensile strength, and strength exhibited a decrease with a temperature of 400°C. This demonstrates that concrete underwent deterioration and damage after reaching a temperature of 400°C.
- Microstructural characteristics are correlated with the mechanical properties of concrete at elevated temperatures. Formation of larger size cracks, voids, and pores are visible from SEM images after 400°C accompanied by decomposition of CSH gel.
- The residual values of compressive strength, peak strain, and modulus of elasticity obtained from the present study are compared with the estimated values from codes and existing experimental results. The comparison indicated inconsistencies between the observed and estimated data, highlighting the significance of the establishment of analytical models for residual properties that are specifically required for no-slump concrete tested in unstressed residual conditions.
- The residual compressive strength, modulus of elasticity, and Poisson's ratio exerted a substantial impact on the structural behaviour of the prestressed hollow core slab, causing the postfire structural elements to become crucial with greater deflection and lower values of stiffness.

Acknowledgements

The authors wish to thank the support of the Centre for Advanced Concrete Research Laboratory (CACR), SRM Institute of Science and Technology, for completing the experimental studies necessary for this research work.

We acknowledge SRM Institute of Science and Technology for high resolution scanning electron microscope (HR-SEM) facility with support from The Ministry of New and Renewable Energy (Project No.31/03/2014-15/PVSE-R&D), Government of India.

References

[1] B.M. Luccioni, M.I. Figueroa, and R.F. Danesi., "Thermo-Mechanic Model for Concrete Exposed to Elevated Temperatures," *Engineering Structures*, vol. 25, no. 6, pp. 729-742, 2003. [CrossRef] [Google Scholar] [Publisher Link]

[2] Zdeněk P. Bažant, M.F. Kaplan, and Zdeněk P. Bazant, *Concrete at High Temperatures: Material Properties and Mathematical Models*, Addison-Wesley, London, England, 1996. [Google Scholar] [Publisher Link]

[3] Gabriel Alexander Khoury, "Effect of Fire on Concrete and Concrete Structures," *Progress in Structural Engineering and Materials*, vol. 2, no. 4, pp. 429-447, 2000. [CrossRef] [Google Scholar] [Publisher Link]

[4] B. Zhang et al., "Residual Fracture Properties of Normal-and High-Strength Concrete Subject to Elevated Temperatures," *Magazine of Concrete Research*, vol. 52, no. 2, pp. 123-136, 2000. [CrossRef] [Google Scholar] [Publisher Link]

[5] I. Hager, "Behaviour of Cement Concrete at High Temperature," *Bulletin of the Polish Academy of Sciences: Technical Sciences*, vol. 61, no. 1, pp. 145-154, 2013. [CrossRef] [Google Scholar] [Publisher Link]

[6] Mervin Ealiyas Mathews et al., "Effect of High-Temperature on the Mechanical and Durability Behaviour of Concrete," *Materials Today: Proceedings*, vol. 42, pp. 718-725, 2021. [CrossRef] [Google Scholar] [Publisher Link]

[7] Daniel Paul Thanaraj et al., "Investigation on Structural and Thermal Performance of Reinforced Concrete Beams Exposed to Standard Fire," *Journal of Building Engineering*, vol. 32, 2020. [CrossRef] [Google Scholar] [Publisher Link]

[8] Venkatesh Kodur, "Properties of Concrete at Elevated Temperatures," *International Scholarly Research Notices*, pp. 1-15, 2014. [CrossRef] [Google Scholar] [Publisher Link]

[9] Dan J. Naus, "*The Effect of Elevated Temperature on Concrete Materials and Structures: A Literature Review*," Technical Report, 2006. [CrossRef] [Google Scholar] [Publisher Link]

[10] Iva Rozsypalova, Pavel Schmid, and Petr Danek, "Determining the Condition of Reinforced and Prestressed Concrete Structures Damaged by Elevated Temperatures," *Procedia Engineering*, vol. 195, pp. 120–126, 2017. [CrossRef] [Google Scholar] [Publisher Link]

[11] Aslani Farhad, "Prestressed Concrete Thermal Behaviour," *Magazine of Concrete Research*, vol. 65, no. 3, pp. 158–171, 2013. [CrossRef] [Google Scholar] [Publisher Link]

[12] Amer Hassan, Mohammed Arif, and M. Shariq, "Mechanical Behaviour and Microstructural Investigation of Geopolymer Concrete after Exposure to Elevated Temperatures," *Arabian Journal for Science and Engineering*, vol. 45, no. 5, pp. 3843-3861, 2020. [CrossRef] [Google Scholar] [Publisher Link]

[13] Bassam A. Tayeh et al., "Effect of Elevated Temperatures on Mechanical Properties of Lightweight Geopolymer Concrete," *Case Studies in Construction Materials*, vol. 15, pp. 1-21, 2021. [CrossRef] [Google Scholar] [Publisher Link]

[14] Abdulrahman Albidah et al., "Behavior of Metakaolin-Based Geopolymer Concrete at Ambient and Elevated Temperatures," *Construction and Building Materials*, vol. 317, 2022. [CrossRef] [Google Scholar] [Publisher Link]

[15] Prasad V. Burle et al., "Post-Fire Investigation on the Mechanical Properties and Physical Characteristics of Fibre-Reinforced Geopolymer Concrete," *Journal of Structural Fire Engineering*, vol. 15, no. 1, pp. 147-174, 2023. [CrossRef] [Google Scholar] [Publisher Link]

[16] Ali Sadrmomtazi, Saeed Haghighat Gashti, and Behzad Tahmouresi, "Residual Strength and Microstructure of Fiber Reinforced Self-Compacting Concrete Exposed to High Temperatures," *Construction and Building Materials*, vol. 230, 2020. [CrossRef] [Google Scholar] [Publisher Link]

[17] T. Rajah Surya et al., "Compressive Strength of Self-Compacting Concrete under Elevated Temperature," *Materials Today: Proceedings*, vol. 40, pp. S83-S87, 2021. [CrossRef] [Google Scholar] [Publisher Link]

[18] Balamurali Kanagaraj et al., "Mechanical Properties and Microstructure Characteristics of Self-Compacting Concrete with Different Admixtures Exposed to Elevated Temperatures," *Jordan Journal of Civil Engineering*, vol. 17, no. 1, pp. 1-9, 2023. [CrossRef] [Google Scholar] [Publisher Link]

[19] Mohamed Amin, Bassam A. Tayeh, and Ibrahim Saad Agwa, "Investigating the Mechanical and Microstructure Properties of Fibre-Reinforced Lightweight Concrete Under Elevated Temperatures," *Case Studies in Construction Materials*, vol. 13, pp. 1-14, 2020. [CrossRef] [Google Scholar] [Publisher Link]

[20] Mehrdad Abdi Moghadam, and Ramezan Ali Izadifard, "Effects of Steel and Glass Fibers on Mechanical and Durability Properties of Concrete Exposed to High Temperatures," *Fire Safety Journal*, vol. 113, 2020. [CrossRef] [Google Scholar] [Publisher Link]

[21] Zhan Guo et al., "Mechanical Properties of Carbon Fiber Reinforced Concrete (CFRC) after Exposure to High Temperatures," *Composite Structures*, vol. 256, 2021. [CrossRef] [Google Scholar] [Publisher Link]

[22] Xin Lyu et al., "Residual Strength of Steel Fibre Reinforced Rubberised UHPC under Elevated Temperatures," *Journal of Building Engineering*, vol. 76, 2023. [CrossRef] [Google Scholar] [Publisher Link]

[23] Mounira Chadli, Nadia Tebbal, and Mekki Mellas, "Impact of Elevated Temperatures on the Behavior and Microstructure of Reactive Powder Concrete," *Construction and Building Materials*, vol. 300, 2021. [CrossRef] [Google Scholar] [Publisher Link]

[24] P. Pliya et al., "The Compressive Behaviour of Natural and Recycled Aggregate Concrete during and after Exposure to Elevated Temperatures," *Journal of Building Engineering*, vol. 38, 2021. [CrossRef] [Google Scholar] [Publisher Link]

[25] Huan Zhang et al., "Models for Uniaxial Stress-Strain Relationship and Thermal Properties of Fine Recycled Aggregate Concrete Exposed to Elevated Temperatures," *Journal of Building Engineering*, vol. 66, 2023. [CrossRef] [Google Scholar] [Publisher Link]

[26] Vadiraj Rao, N. Suresh, and G.P. Arun Kumar, "Studies on the Post Cracking Behaviour of Recycled Aggregate Concrete Beams at Elevated Temperature," *Journal of Structural Fire Engineering*, vol. 14, no. 4, pp. 501-521, 2023. [CrossRef] [Google Scholar] [Publisher Link]

[27] ACI 116R-00, Cement and Concrete Terminology, American Concrete Institute, 2000. [Online]. Available: https://www.studocu.com/row/document/jamaa%D8%A9-tshryn/image-processing/aci-116r-00-cement-and-concrete-terminology/52989770

[28] ACI 211.3R-02, Guide for Selecting Proportions for No-Slump Concrete, American Concrete Institute, 2002. [Online]. Available: https://www.concrete.org/store/productdetail.aspx?ItemID=211302&Format=DOWNLOAD&Language=English&Units=US_AND_METRIC

[29] Long T. Phan, and Nicholas J. Carino, "Fire Performance of High Strength Concrete: Research Needs," *Advanced Technology in Structural Engineering*, pp. 1-8, 2012. [CrossRef] [Google Scholar] [Publisher Link]

[30] Tudor Petrina, "Fire Structural Analysis According to European Codes," *Acta Technica Napocensis: Civil Engineering & Architecture*, vol. 54, no. 3, pp. 308-317, 2011. [Google Scholar]

[31] K. Sakr, and E. EL-Hakim., "Effect of High Temperature or Fire on Heavy Weight Concrete Properties," *Cement and Concrete Research*, vol. 35, no. 3, pp. 590-596, 2005. [CrossRef] [Google Scholar] [Publisher Link]

[32] Marta Castellote et al., "Composition and Microstructural Changes of Cement Pastes Upon Heating, as Studied by Neutron Diffraction," *Cement and Concrete Research*, vol. 34, no. 9, pp. 1633-1644, 2004. [CrossRef] [Google Scholar] [Publisher Link]

[33] Gai-Fei Peng, and Zhi-Shan Huang, "Change in Microstructure of Hardened Cement Paste Subjected to Elevated Temperatures," *Construction and Building Materials*, vol. 22, no. 4, pp. 593-599, 2008. [CrossRef] [Google Scholar] [Publisher Link]

[34] G. Khoury et al., *Fire Design of Concrete Structures-Materials, Structures and Modelling*, International Federation for Structural Concrete (fib) CEB-FIP, Monograph or Scientific Treatise, 2007. [Google Scholar] [Publisher Link]

[35] A. Savva, P. Manita, and K.K. Sideris, "Influence of Elevated Temperatures on the Mechanical Properties of Blended Cement Concretes Prepared with Limestone and Siliceous Aggregates," *Cement and Concrete Composites*, vol. 27, no. 2, pp. 239-248, 2005. [CrossRef] [Google Scholar] [Publisher Link]

[36] W. Khaliq, and V.K.R. Kodur, "Effect of High Temperature on Tensile Strength of Different Types of High-Strength Concrete," *ACI Materials Journal*, vol. 108, no. 4, pp. 394-402, 2011. [CrossRef] [Google Scholar] [Publisher Link]

[37] IS: 516-1959, Indian Standard: Methods of Tests for Strength of Concrete, Bureau of Indian Standards, New Delhi, 1959. [Online]. Available: https://law.resource.org/pub/in/bis/S03/is.516.1959.pdf

[38] ASTM C469/C469M-14, Standard Test Method for Static Modulus of Elasticity and Poisson's Ratio of Concrete in Compression, ASTM International, 2014. [Online]. Available: https://www.concrete.org/publications/internationalconcreteabstractsportal/m/details/id/51738434

[39] Ulrich Schneider, "Concrete at High Temperatures – A General Review," *Fire Safety Journal*, vol. 13, no. 1, pp. 55–68, 1988. [CrossRef] [Google Scholar] [Publisher Link]

[40] EN 1992-1-2, Eurocode 2: Design of Concrete Structures-Part 1-2: General Rules – Structural Fire Design, CEN, Brussels, 2004. [Online]. Available: https://www.phd.eng.br/wp-content/uploads/2015/12/en.1992.1.2.2004.pdf

[41] ACI 216.1, Code Requirements for Determining Fire Resistance of Concrete and Masonry Construction Assemblies, American Concrete Institute, 2014. [Online]. Available: https://www.concrete.org/Portals/0/Files/PDF/Previews/216_1-14.PREVIEW.pdf

[42] ASCE, Structural Fire Protection, ASCE Manuals and Reports on Engineering Practice No. 78, T. T. Lie, Ed., American Society of Civil Engineers, New York, 1992. [Online]. Available: https://ascelibrary.org/doi/10.1061/9780872628885

[43] Harun Tanyildizi, and Ahmet Coskun, "The Effect of High Temperature on Compressive Strength and Splitting Tensile Strength of Structural Lightweight Concrete Containing Fly Ash," *Construction and Building Materials*, vol. 22, no. 11, pp. 2269-2275, 2008. [CrossRef] [Google Scholar] [Publisher Link]

[44] Abid Nadeem, Shazim Ali Memon, and Tommy Yiu Lo, "The Performance of Fly Ash and Metakaolin Concrete at Elevated Temperatures," *Construction and Building Materials*, vol. 62, pp. 67-76, 2014. [CrossRef] [Google Scholar] [Publisher Link]

[45] Manisha Malik, S.K. Bhattacharyya, and Sudhirkumar V. Barai, "Microstructural Changes in Concrete: Postfire Scenario," *Journal of Materials in Civil Engineering*, vol. 33, no. 2, 2019. [CrossRef] [Google Scholar] [Publisher Link]

[46] Jianzhuang Xiao, and Gert König, "Study on Concrete at High Temperature in China an Overview," *Fire Safety Journal*, vol. 39, no. 1, pp. 89-103, 2004. [CrossRef] [Google Scholar] [Publisher Link]

[47] Long-yuan Li, and John Purkiss, "Stress–Strain Constitutive Equations of Concrete Material at Elevated Temperatures," *Fire Safety Journal*, vol. 40, no. 7, pp. 669-686, 2005. [CrossRef] [Google Scholar] [Publisher Link]

[48] Y.F. Chang et al., "Residual Stress-Strain Relationship for Concrete after Exposure to High Temperatures," *Cement and Concrete Research*, vol. 36, no. 10, pp. 1999-2005, 2006. [CrossRef] [Google Scholar] [Publisher Link]

[49] ACI 318-11, Building Code Requirements for Structural Concrete and Commentary, American Concrete Institute, American Concrete Institute, 2011. [Online]. Available: https://www.pecivilexam.com/Study_Documents/Struc-Materials-Online/ACI_318-Building-Code-2011.pdf

[50] B. Georgali, and P.E. Tsakiridis, "Microstructure of Fire-Damaged Concrete. A Case Study," *Cement and Concrete composites*, vol. 27, no. 2, pp. 255-259, 2005. [CrossRef] [Google Scholar] [Publisher Link]

[51] IS 10262: 2009, Indian Standard: Concrete Mix Proportioning-Guidelines, Bureau of Indian Standards, New Delhi, 2009. [Online]. Available: https://law.resource.org/pub/in/bis/S03/is.10262.2009.pdf